nature structural & molecular biology

Structural insights into FtsZ protofilament formation

Maria A Oliva[1,2], Suzanne C Cordell[1] & Jan Löwe[1]

The prokaryotic tubulin homolog FtsZ polymerizes into a ring structure essential for bacterial cell division. We have used refolded FtsZ to crystallize a tubulin-like protofilament. The N- and C-terminal domains of two consecutive subunits in the filament assemble to form the GTPase site, with the C-terminal domain providing water-polarizing residues. A domain-swapped structure of FtsZ and biochemical data on purified N- and C-terminal domains show that they are independent. This leads to a model of how FtsZ and tubulin polymerization evolved by fusing two domains. In polymerized tubulin, the nucleotide-binding pocket is occluded, which leads to nucleotide exchange being the rate-limiting step and to dynamic instability. In our FtsZ filament structure the nucleotide is exchangeable, explaining why, in this filament, nucleotide hydrolysis is the rate-limiting step during FtsZ polymerization. Furthermore, crystal structures of FtsZ in different nucleotide states reveal notably few differences.

FtsZ is a key molecule of bacterial cell division, forming a filamentous ring that constricts when the cell divides. Its role in division is, at least partly, to recruit several other proteins to the division site. In *Escherichia coli*, for example, they are recruited in sequential order: FtsA/ZipA, FtsK, FtsQ, FtsL/FtsB, FtsW, FtsI, FtsN and AmiC[1–4]. Early sequence comparisons indicated FtsZ might be related to eukaryotic tubulin and *in vitro* studies showed it could polymerize in a GTP-dependent manner akin to that of tubulin[5]. The three-dimensional structures of *Methanococcus jannaschii* FtsZ (MjFtsZ, GDP-bound, PDB entry 1FSZ)[6] and eukaryotic α/β tubulin[7] indeed show them to be closely related[8]. Both proteins contain two globular domains, an N-terminal GTP-binding domain and a C-terminal domain. Tubulin has two additional large C-terminal helices that lie on the outer microtubule surface[9] and are thought to be the main interaction site for motor proteins and other proteins able to bind microtubules.

The tubulin structure was solved in its polymerized state in flat zinc-induced sheets, providing information about the longitudinal interaction. The tubulin protofilament is formed by the interaction of the C-terminal domain of one subunit with the GTP-binding N-terminal domain of another, producing a completely straight one-dimensional polymer. Notably, GTPase activity is switched on when tubulin polymerizes owing to the insertion of a key residue for catalysis (Glu254) into the GTP-binding pocket of the preceding subunit[8]. The equivalent residue in β-tubulin is a lysine, resulting in a nonhydrolyzed GTP bound to α-tubulin at all times (N site). The loop containing this critical residue has been termed loop T7 (ref. 8), as it is the seventh loop surrounding the nucleotide in the polymerized protein. Loops T1–T6 are part of the GTP-binding pocket on one side of the molecule; T7 is located on the opposite side and comes into contact with nucleotide only when the protein is in a polymer.

Because FtsZ and tubulin are closely related, it has always been assumed that FtsZ would form similar protofilaments to those formed by tubulin. Several pieces of evidence support this: FtsZ polymerizes with a longitudinal subunit repeat very similar (40 Å in tubulin, 42–43 Å in FtsZ) to that of tubulin protofilaments[10,11]; an FtsZ protofilament modeled on the tubulin structure fits very well into a low-resolution map of FtsZ calcium-induced sheets[12]; a mutant of the residue corresponding to tubulin's Glu254 in FtsZ (*E. coli* Asp212 or *M. jannaschii* Asp238) abolishes GTPase activity[13] and the SOS cell division inhibitor SulA binds to the T7 loop, stopping the protein from polymerizing[14].

Recently, it has been shown that one notable difference between FtsZ and tubulin is in the GTPase reaction kinetics[15]. Tubulin hydrolyzes GTP very quickly upon polymerization, but nucleotide exchange is slow or nonexistent in the polymer. Hence, the polymer is mostly GDP-bound, with the GTP-containing tubulin subunits forming a cap at the fast-growing (+)-end. This state is not thermodynamically stable and the whole polymer will eventually collapse (due to the dynamic instability of microtubules)[16]. The tubulin protofilament structure actually explains this, as the nucleotide is completely occluded from the solvent, preventing nucleotide release. Conversely, the rate-limiting step for FtsZ seems to be hydrolysis and not nucleotide exchange[15], resulting in a polymer that is mostly GTP-bound[15,17,18]. These data are incompatible with dynamic instability. Moreover, there are currently no data available clearly demonstrating the existence of dynamic instability for FtsZ.

In vitro, FtsZ can form many different lateral interactions depending on the conditions used[11,19,20] but nothing is known about the exact nature of FtsZ filaments *in vivo*. The *in vivo* polymer in the Z ring at midcell may consist of one or several single protofilaments, a double filament, a bundle or a helix that can change its pitch[21].

Both tubulin and FtsZ show nucleotide-dependent changes to the curvatures of their protofilaments. This is important for tubulin because the change from GTP-bound straight to GDP-bound curved

[1]MRC Laboratory of Molecular Biology, Hills Road, Cambridge CB2 2QH, UK. [2]Present address: Centro de Investigaciones Biológicas (CIB-CSIC), c/ Ramiro de Maeztu, 9, 28040 Madrid, Spain. Correspondence should be addressed to J.L. (jyl@mrc-lmb.cam.ac.uk).

Published online 21 November 2004; doi:10.1038/nsmb855

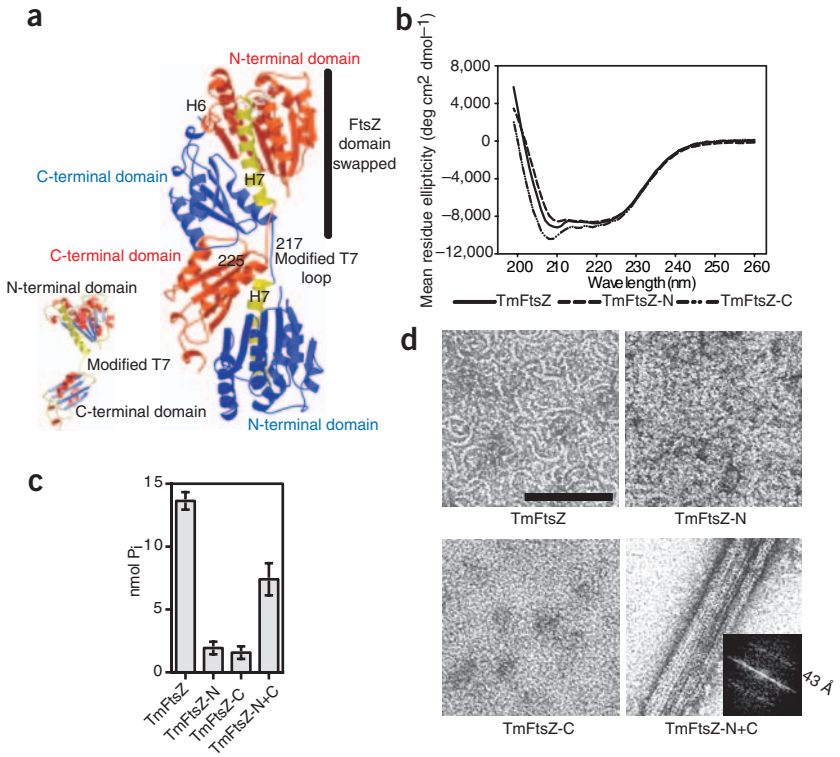

Figure 1 FtsZ consists of two independent domains that can recombine noncovalently. (**a**) Crystallized *T. maritima* FtsZ protein has a modified T7 loop with two extra residues and three mutated residues (amino acid sequence IRLTSRFARIE replacing INLDXXFADIE, starting at residue 217). This probably causes the N- and C-terminal domains to become less tightly associated. The protein crystallizes as a domain-swapped dimer with one FtsZ molecule formed from two separate chains (chain A, blue; chain B, red; both helices H7, yellow). The small insert shows the structure of one chain only. (**b**) CD spectra of TmFtsZ full-length, N- and C-terminal domains showing all three to be folded proteins. (**c**) Malachite green GTPase assay. Combining TmFtsZ N- and C-terminal domains restores the GTPase activity of FtsZ. (**d**) Electron micrographs of full-length and isolated as well as combined N- and C-terminal domains. The isolated domains don't polymerize (top right and bottom left), but when combined they do (bottom right). Full-length TmFtsZ produces predominantly curved protofilaments (top left), whereas the combined domains produce straight bundles with a longitudinal repeat of ~43 Å (bottom right). Bar, 100 nm.

protofilaments might provide the energy for dynamic instability. Likewise, FtsZ protofilaments formed with GTP are straight, and those formed with GDP are curved[22]. However, this may be less significant in the FtsZ case because *in vivo* protofilaments are predicted not to exist in the GDP state for very long.

Here, we provide direct proof that FtsZ and tubulin form equivalent longitudinal contacts in their protofilaments with the crystal structure of an FtsZ dimer. To investigate any conformational changes during the GTPase cycle, we crystallized the MjFtsZ mutant W319Y (GTPase deficient)[23] and MjFtsZ with GMPCPP. Furthermore, *Thermotoga maritima* FtsZ with a modified T7 loop crystallizes as a domain-swapped dimer. This, together with biochemical evidence on the isolated domains, demonstrates that the N- and C-terminal domains of FtsZ are two independent folding entities, possibly suggesting that earlier in evolution they were two independent proteins.

RESULTS

FtsZ consists of two independent domains

To obtain an FtsZ protein that is incapable of polymerization and GTP hydrolysis, several residues in the T7 loop of *T. maritima* FtsZ (TmFtsZ) were mutated, resulting in the amino acid sequence IRLTSRFARIE, replacing INLDXXFADIE (where X is any residue) starting at residue 217. Originally, these changes were introduced for an unrelated experiment to obtain a completely polymerization-deficient TmFtsZ. The structure with GMPCPP, solved by molecular replacement using the *M. jannaschii* (Mj) FtsZ crystal structure (PDB entry 1FSZ)[6] at a resolution of 2.0 Å, contains two molecules in the asymmetric unit (**Table 1**). Notably, the protein crystallized as a domain-swapped dimer, with the N-terminal domain of chain A forming an FtsZ molecule with the C-terminal domain of chain B and vice versa (**Fig. 1a**).

The resulting FtsZ molecules are quite similar to the MjFtsZ structure (PDB entry 1FSZ, apart from the domain swap), with an r.m.s. deviation between the N- and C-terminal domains of FtsZ from the two organisms of ~1 Å. The sequence of TmFtsZ has no helix H0 and the last two strands of MjFtsZ are replaced by a small helix. Overall, the r.m.s. deviation is 1.9 Å with 87% of all residues aligned in MjFtsZ and 92% in TmFtsZ made from two different chains (sequence identity is 46%). The larger overall r.m.s. deviation is the result of a slight movement of the C-terminal domain in TmFtsZ when compared with MjFtsZ. The only significant conformational change when comparing MjFtsZ and TmFtsZ is in the loop between H6 and H7, but that is most likely caused by an extra residue in the *T. maritima* protein at this position. All T loops superimpose very well, despite the fact that TmFtsZ was crystallized in the triphosphate state and is unable to hydrolyze.

The fact that the domain swap is possible and a report describing two-stage unfolding kinetics of FtsZ[24] prompted us to test whether the N- and C-terminal domains of FtsZ are independently folding entities and whether the two domains made as separate proteins can reconstitute functional FtsZ in a GTPase and polymerization assay. FtsZ-N (residues 22–190, C-terminal His_6-tag) and FtsZ-C (residues 188–366, C-terminal His_6-tag) were expressed and purified under native conditions (**Supplementary Fig. 1** online). In these constructs, H7 is located on the C-terminal domain, as the C-terminal domain becomes unstable otherwise (data not shown). In contrast, H7 stays with the N-terminal domain in the TmFtsZ domain-swapped structure (**Fig. 1a**). However, the isolated FtsZ-C domain exposes many additional surfaces that are shielded by the N-terminal domain in the domain-swap structure and H7 seems to be required for the stability of an isolated C-terminal domain.

Both TmFtsZ domains were well expressed and were well-behaved proteins when purified (**Supplementary Fig. 1** online); folding was demonstrated using CD spectra (**Fig. 1b**). The two isolated domains had no GTPase activity whereas the two domains combined showed significant GTPase activity (**Fig. 1c**). Finally, the combined N- and C-terminal domains polymerized into genuine FtsZ protofilaments with the characteristic longitudinal repeat of 43 Å (**Fig. 1d**). In fact, full-length TmFtsZ produced only short, bent protofilaments, probably because of the consumption of GTP under these conditions

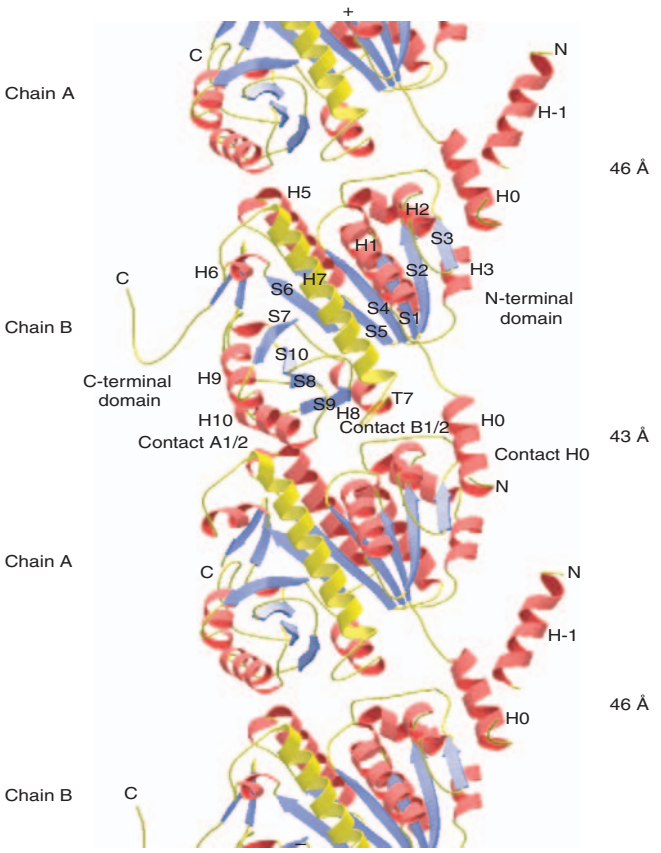

Figure 2 Crystal structure of a semicontinuous FtsZ protofilament. Refolded *M. jannaschii* FtsZ, nucleotide-free, crystallizes as a dimer closely resembling the α/β tubulin dimer with a subunit spacing of ~43 Å. The crystal packing shows the tight 43-Å noncrystallographic dimer of FtsZ in the middle, with less tightly packed subunits on top and at the bottom, in an arrangement very close to a continuous protofilament in the crystals.

(**Fig. 1d**, top left). The combined domains produced large, straight bundles of filaments, probably because of reduced GTPase activity (**Fig. 1d**, bottom right). From these experiments and the domain-swapped dimer we conclude that the N- and C-terminal domains of FtsZ have retained independent folding capacities and can be regarded as fully separate domains.

Nucleotide-free FtsZ protofilament-like dimer

To obtain nucleotide-free MjFtsZ, the protein first has to be unfolded and the nucleotide washed away; then the protein is refolded with high efficiency[24] (see Methods). The resulting FtsZ is nucleotide-free, as judged by a spectrophotometric assay (data not shown). The protein was crystallized without adding nucleotide or magnesium. The structure was solved by molecular replacement using the published structure (PDB entry 1FSZ).

The nucleotide-free MjFtsZ protein crystallizes as a semicontinuous protofilament (**Fig. 2**) closely resembling the orientation and stacking seen in polymerized tubulin (PDB entry 1JFF; **Fig. 3**)[25] and is very similar to the protofilament model derived by EM of polymerized, calcium-induced MjFtsZ sheets[12]. The arrangement in the crystals is semicontinuous with the subunit spacing alternating between 43.2 Å and 46.4 Å. The 46-Å distance is too large for a proper protein-protein interface, producing a gap (**Fig. 2**). The break in the protofilament is necessary for crystallization because the dimer formed by the 43-Å interaction (middle of **Fig. 2**) is not completely straight (**Fig. 3d**,**e**), forcing every second contact to be broken because of a bend of ~10°.

The dimer interface of the 43-Å contact is tight (**Fig. 3c**, 1,011 Å^2, 8% of FtsZ's surface) and the packing probably represents true protofilament interactions with only minor distortions. The 43-Å spacing is very close to the 42.6-Å spacing observed in electron micrographs of polymerized MjFtsZ[12] and the 42–43 Å seen for polymerized *E. coli* and *M. jannaschii* FtsZ[10,11]. It is longer than the 40-Å distance observed in microtubules and tubulin zinc sheets, but tubulin assembly in the GTP state with GMPCPP produces a subunit spacing of 42–43 Å (ref. 26).

The MjFtsZ protofilament dimer forms via three interacting regions (named A, B and H0, see **Supplementary Table 1** online; naming convention is similar to that in ref. 27) both on the upper and lower subunits (**Figs. 2–4**). The upper (+)-end subunit (chain B) uses H0, T7, H8, S9 and H10 for the interaction, and the lower (–)-end subunit uses loops H2, S3, T3 and T5 (the loop between H6 and H7). Notably, H0 changes its position when compared with the monomeric form of FtsZ (PDB entry 1FSZ) and becomes an integral part of the protofilament contact. The movement of H0 had actually been predicted from our earlier calcium sheets–derived protofilament model. There is also weak density for residues 1–21 present in the dimeric MjFtsZ structure, which is difficult to model. These residues form a helix that we have named H-1.

Notably, apart from H0, all contacts in the upper subunit reside in the C-terminal domain, whereas all contacts in the lower subunit come from the N-terminal domain. Helix H0 is not conserved in most FtsZ proteins (including *T. maritima* FtsZ (**Fig. 1**) and *P. aeruginosa* FtsZ[14]).

Activation of the attacking water molecule

We soaked GTP and GTP with Mg^{2+} into the preformed crystals of MjFtsZ protofilaments. GDP soaks failed because the crystals stopped diffracting and dissolved. Also, the crystals had to be frozen fairly quickly, most likely because of slow hydrolysis of the GTP. There are no significant conformational changes in the protein with soaked in GTP or MgGTP. The resulting structures of the triphosphate soaks show for the first time the complete FtsZ GTPase active site with two key residues in T7 complementing the N-terminal GTP-binding domain of FtsZ (**Fig. 4**): Asp235 and Asp238 are positioned in good hydrogen bonding distance (OD-Asp238 to O-Wat105, 2.8 Å; OD-Asp235 to O-Wat105, 3.5 Å) to polarize Wat105, which is the attacking water molecule for the GTP γ-phosphate hydrolysis reaction. The γ-phosphate is further polarized using the magnesium ion in complex with Gln75, several waters and the γ- and β-phosphates.

Lack of conformational changes

Superposition of the nucleotide-free MjFtsZ structure with the GDP-bound structure highlighted very few differences. We replaced GDP in the $I2_13$ MjFtsZ crystal form by soaking in GMPCPP. The resulting structure at a resolution of 2.5 Å clearly shows the triphosphate nucleotide with the γ-phosphate-contacting loop T3 (**Fig. 5a**). However, soaking in nucleotide might not show the anticipated conformational changes. To circumvent this problem, we crystallized a GTPase-deficient MjFtsZ mutant (W319Y) that is unable to hydrolyze GTP and forms very stable polymers[10,23]. We crystallized the mutant protein in a space group different from the previous one for the GDP-bound protein or the nucleotide-free protein, eliminating the possibility that the protein would be locked into one conformation. The structure is of somewhat lower quality, caused by disorder of six of the nine molecules in the asymmetric unit. However, the density is very good for three molecules (chains B, E and H; electron density shown in **Supplementary Fig. 2** online). In our structure of the FtsZ protofilament, Trp319 is positioned above the base of the nucleotide, but is too far away for a direct interaction (~8.5 Å

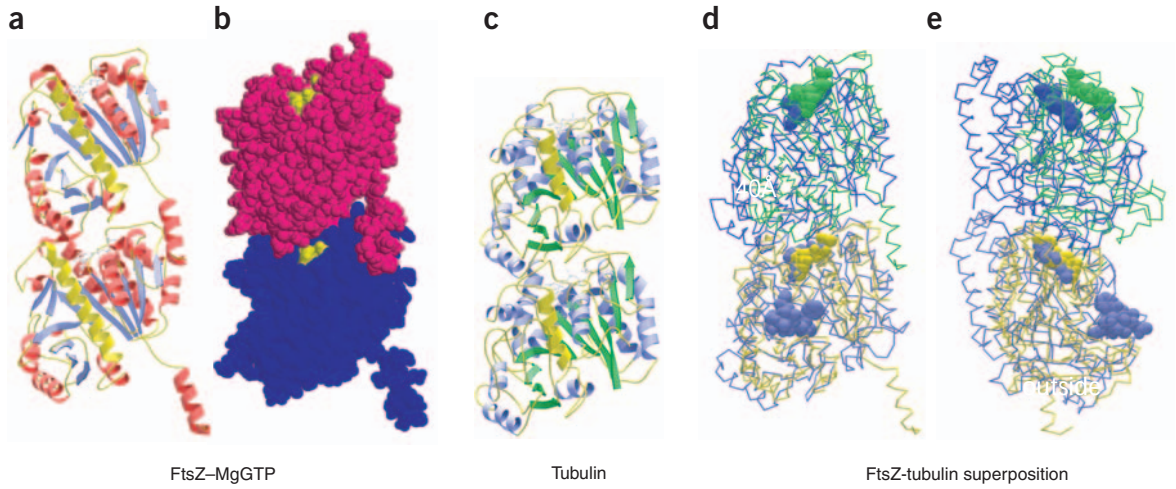

Figure 3 Structure of the FtsZ dimer. (**a**) FtsZ dimer obtained from nucleotide-free MjFtsZ, with MgGTP soaked in after crystallization. (**b**) The two subunits form a tight dimer but the nucleotide-binding site (yellow) is accessible from the outside and the nucleotide is not completely surrounded by protein. An open channel with approximate dimensions of 8 × 9 Å connects the active site with surrounding solvent. MgGTP can be soaked into the preformed filament, demonstrating that the nucleotide can freely exchange. (**c**) The dimer arrangement in FtsZ closely resembles the α/β tubulin dimer observed in tubulin zinc sheets (PDB entry 1JFF)[25]. The subunit spacing is shorter in GDP tubulin (40 Å, tubulin; 42–43 Å, FtsZ)[26]. (**d**,**e**) Superposition of the FtsZ and tubulin dimers (tubulin, blue; FtsZ, green). Nucleotides are in similar colors as space-filling models, as is taxol bound to β-tubulin. The two lower subunits were superimposed, highlighting a rotation of ~10° of the upper subunit in the FtsZ dimer when compared with tubulin. The rotation is mostly into the inside of the microtubule.

from indole to purine). We can only speculate that this mutant is inactive because the additional hydroxyl group disturbs the water network within the active site cavity.

When all available structures of MjFtsZ are superimposed (**Fig. 5b**), a notable picture emerges: there are very few differences between the empty, GDP and GTP states. This is true both locally (backbone conformations) and globally (domain movements). The three different nucleotide states all crystallized in different packing environments. Only minor changes are observed in loop T2 and in the loop connecting H6 and H7; however that loop is part of crystal contacts in at least two structures and might have slightly moved because of crystal packing. T3, however, is very similar in all three states, contrary to expectations[23].

DISCUSSION

The same protofilament is formed by FtsZ and tubulin

Previously, only low-resolution information from three-dimensional electron crystallography and manual docking was available for the FtsZ protofilament structure[12]. We set out to crystallize FtsZ in its polymerized state, but crystallizing FtsZ in the presence of GTP or analogs is probably not possible. The polymerization rate of FtsZ is much faster than the rate of crystal growth. In addition, a published GTPase-deficient mutant of MjFtsZ, W319Y, crystallized only as a monomer in our studies. To circumvent these problems, we used nucleotide-free FtsZ because the empty state should be closest in structure to the triphosphate state and is able to polymerize[28].

Using nucleotide-free MjFtsZ, we produced a structure that shows protofilament contacts markedly similar to those of tubulin filaments (**Figs. 2** and **4a**,**b**). This provides direct evidence that FtsZ and tubulin polymerize into very similar protofilaments.

However a tilt of ~10° is apparent in the FtsZ dimer (**Fig. 3e**). A recent structure of two tubulin dimers bound to stathmin[29] shows considerable bending both at the interdimer and at the intersubunit interfaces. The stathmin-induced bending (12° for each of the α and β subunits) of the tubulin subunits is thought to be the reason for stathmin's microtubule-interrupting activity. The stathmin-induced curvature of the tubulin protofilament is tangential to the microtubule wall and is probably different from the bend in GDP-bound tubulin rings, which is thought to be to the outside[30]. Notably, our FtsZ dimer is bent to the inside of the microtubule (**Fig. 3e**) when FtsZ is aligned with tubulin in microtubules. It is not known, however, which way FtsZ-GDP protofilaments bend.

Evolutionary origin of the two FtsZ domains

We have provided biochemical evidence that the N- and C-terminal domains of FtsZ fold independently and are stable on their own. Combined in solution, they associate noncovalently into an FtsZ molecule and are capable of GTP hydrolysis coupled to protofilament formation. These data become relevant when taken together with the structure of the FtsZ protofilament contact showing that apart from H0, which is an uncommon extension to MjFtsZ, all contacts at the longitudinal filament interface are made between the N- and C-terminal domains. No contacts exist between two N- or C-terminal domains along the filaments, apart from H0.

This suggests a model that describes how FtsZ and tubulin polymerization developed during evolution (**Supplementary Fig. 3** online). The C-terminal domain complements the GTP-binding pocket of the GTP-binding domain by providing two water-polarizing residues (Asp235 and Asp238). We speculate that this was the original function of the C-terminal domain when it might have been an independent protein earlier in evolution. The resulting domain-fused molecule associates into a linear polymer based on the domain interactions and has a polymerization-dependent activation mechanism because polymerization involves the interaction of a GTP-binding domain (N-terminal) and its GTPase-complementing domain (C-terminal).

The N-terminal domains of tubulin and FtsZ are closely related to the very common Rossmann fold of ATPases, and the C-termi-

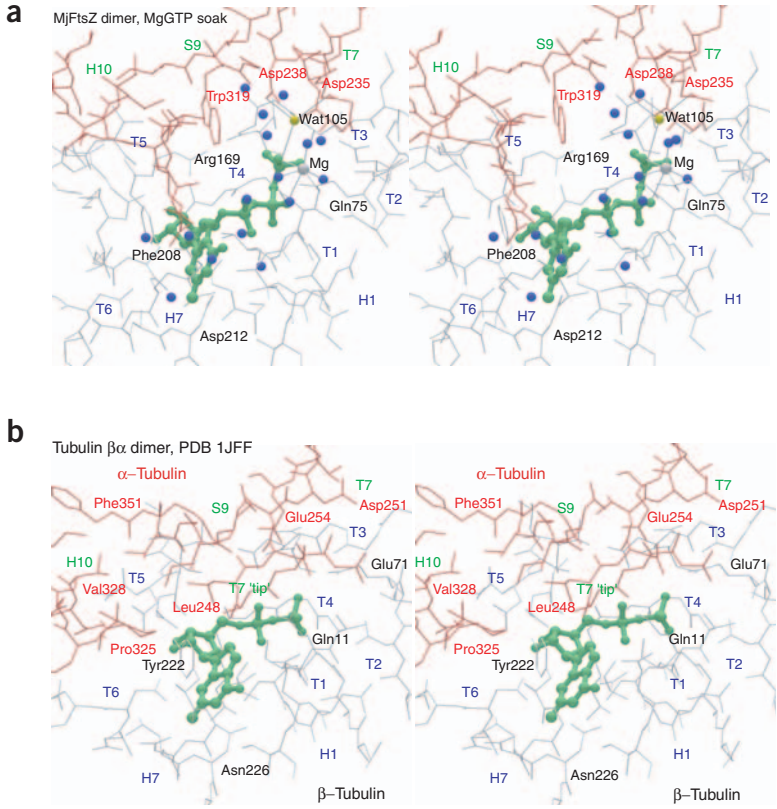

Figure 4 Detailed view of the intersubunit active sites in MjFtsZ and tubulin. (**a**) FtsZ dimer. The GTPase domain of the lower subunit is complemented by two aspartates (Asp235 and Asp238) that polarize the attacking water molecule (Wat105). Apart from these residues, which belong to loop T7, S9 and helix H10 of the C-terminal domain of FtsZ are involved in the protofilament contact. (**b**) α/β tubulin (PDB entry 1JFF) with α-tubulin on top (not the tubulin solution dimer, but the catalytically active contact formed in protofilaments). The general arrangement in the active site is very similar to that of FtsZ with T7, S9 and H10 of the C-terminal (intermediate) domain making the protofilament contact. Very little space would be left for a γ-phosphate, and the polarizing acidic residue, Glu254, is not in the right position to polarize the attacking water molecule. The tubulin structure was solved at low resolution and exact side chain positions may not be known for all residues.

nal domain has several structural homologs in the SCOP database (chorismate mutase-like), showing that similar domains exists on their own in modern organisms and supporting our idea.

The GTPase switch

We show here that FtsZ switches its GTPase activity between the off state (monomer) and the on state (polymer) by complementing the GTP-binding pocket with two water-polarizing residues that are in direct contact with the attacking water molecule for γ-phosphate hydrolysis. From the structural data it seems that the FtsZ GTPase switch stabilizes an early transition state in which the attacking water molecule becomes polarized. The GTP-binding domain of FtsZ contains its own 'arginine finger' (MjFtsZ: Arg169, **Fig. 4a**) that is required for efficient catalysis as it stabilizes the charge that develops during a later transition state. How is FtsZ's activation mechanism related to others? A large variety of NTPase-activating mechanisms exist in nature and it seems possible to accelerate nucleotide hydrolysis in various ways by stabilizing different transition states. Many classic small GTPase-activating proteins (GAPs) use a so-called arginine finger that reaches into the active site, most likely stabilizing the charge produced during nucleotide hydrolysis[31]. However, recent data suggest that this mechanism is not universal[32]. The nitrogenase iron protein dimer[33], which is also related to the SRP heterodimeric GTPase complex between Ffh and FtsY, again brings a positively charged lysine or arginine residue close to the phosphates most likely to compensate for the charge of the transition state[34,35]. In all of these complexes, the water-polarizing residue resides in the GTP-binding domain. In the complex of $G_{i\alpha1}$ with activator RGS4 there seems to be another variation with a water-polarizing asparagine (Asn128) and a binding surface that helps the GTP-binding domain through its transition state[36].

Freely accessible nucleotide in the FtsZ protofilament

Overall, the FtsZ GTPase site assembled from two subunits in the protofilament is very similar to tubulin's, with the corresponding residues producing the protofilament contacts (**Fig. 4a**,**b**). H0 is absent in tubulin and the contact seems to be replaced by an extension (approximately residues 25–60 in tubulin[7]) in the N-terminal domain (**Fig. 3d**) that produces another intersubunit contact. In tubulin protofilaments, the nucleotides bound to α- and β-tubulin are completely occluded by the protein, making disassembly essential for nucleotide exchange. This means that nucleotide exchange is the rate-limiting step and creates dynamic instability of microtubules in which the tubulin polymers exist in the GDP-bound form with a GTP cap. In our FtsZ dimer structure, the nucleotide is far from completely occluded and exchange is possible while the protein is in the protofilament, as we have demonstrated by soaking it in nucleotide. The opening giving access to the nucleotide in the active site is large enough for free diffusion of a GTP, with dimensions of approximately 8 × 9 Å. Notably, this provides a structural explanation for the previous finding that GTP hydrolysis and not exchange is the rate-limiting step for FtsZ[15,17] GTP hydrolysis.

Alternatively, the state we are looking at in the FtsZ dimer structure could also represent a prehydrolysis conformation, and after γ-phosphate release or hydrolysis the active site may close. This idea is somewhat supported by the differences between the positions of Asp251 and Glu254 (**Fig. 4b**), the residues presumed to polarize the attacking water in tubulin. In the tubulin structure, they are not in the correct position for attack (although resolution of the tubulin structure is low at 3.5 Å and the position of side chains might not be very accurate) and overall there is not enough space for a γ-phosphate and an attacking water molecule, indicating that a conformational transition has occurred after γ-phosphate release. A change in subunit

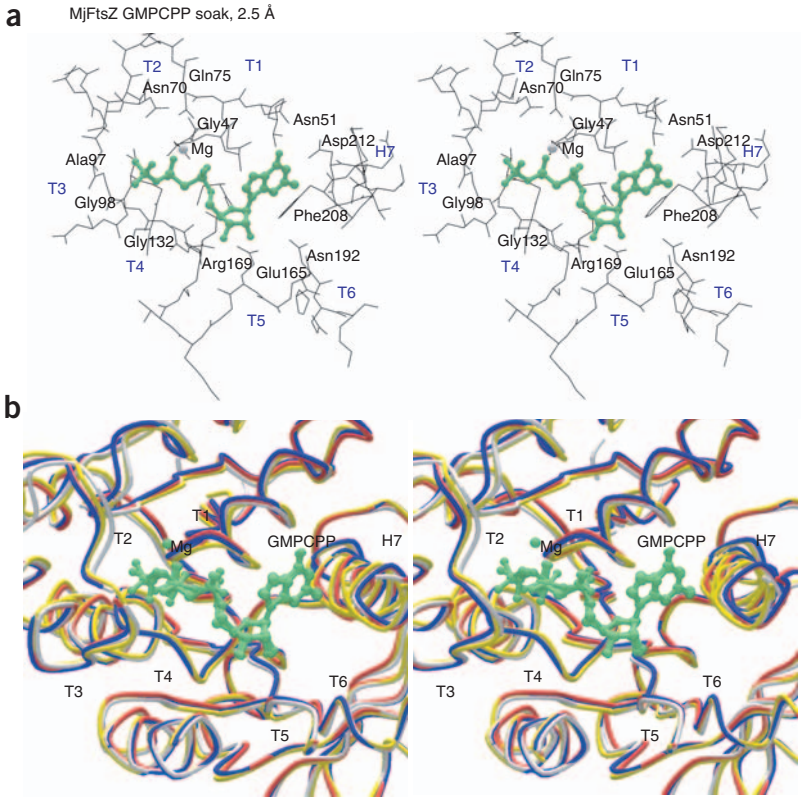

Red MjFtsZ, monomer, GDP, 2.8 Å, *I*213
Blue MjFtsZ, monomer, GMPCPP, 2.5 Å, soaked into *I*213
White MjFtsZ W319Y, monomer, GTP, 3.0 Å, $P3_1$ (*P*1)
Yellow MjFtsZ, protofilament, empty, 2.7 Å, $P2_1$

Figure 5 A lack of conformational changes in different FtsZ structures. (**a**) *M. jannaschii* FtsZ with bound GMPCPP at a resolution of 2.5 Å. GDP-containing crystals were soaked with magnesium and GMCPP in a special buffer to replace the bound nucleotide. The γ-phosphate occupies the previously identified binding pocket[6], making hydrogen bonding contacts to loop T3. (**b**) Superposition of *M. jannaschii* FtsZ active sites: minimal changes are observed between the structures of monomers containing nucleotides and the refolded, empty monomer in completely different space groups and packing arrangements. Stereo drawing.

spacing has been observed previously in the formation of polymers of tubulin[26].

A lack of conformational changes

We superimposed several structures of FtsZs from three organisms and in three different nucleotide states, all in different crystal-packing arrangements. Notably, very few conformational changes were detected (**Fig. 5b**). One possible reason for the lack of conformational differences between the di- and triphosphate structures of FtsZ is that the GDP MjFtsZ structure is not in the GDP state, because the protein initially has some GTP bound to it (MjFtsZ purifies with ~60% GDP and ~40% GTP bound[10]. If GDP–FtsZ does not crystallize, then there is selection for GTP–FtsZ in the crystals and the nucleotide could slowly hydrolyze after the crystals have formed. The lack of conformational changes in FtsZ between different nucleotide states is also reflected in the fact that the two other FtsZ proteins from *T. maritima* (GMPCPP, this study) and *P. aeruginosa* GTP and GDP[14] show only very small changes in the conformation of the T loops or the domain arrangements despite having only moderate sequence similarity (data not shown).

If we assign all available structures of MjFtsZ to a very simple polymerization cycle of FtsZ it becomes clear that at least one major state is still missing (**Supplementary Fig. 4** online) and the conformational change might occur after or during hydrolysis of the nucleotide when in the filament. One would have to propose, however, that when depolymerized, the protein switches back to the observed conformation of MjFtsZ–GDP. This idea is supported by the fact that when we added GDP or Mg^{2+}GDP to the empty MjFtsZ dimer crystals, they stopped diffracting instantly and dissolved. Because hydrolysis, not exchange of nucleotide, is rate-limiting, it is unlikely that the conformational change induces long-lasting changes in the polymer in the bacterial cell as it will be mostly GTP-bound due to the high intracellular GTP concentration[15].

METHODS

General crystallography. We used a 100-nl crystallization setup in our laboratory with 1,500 standard conditions[37]. Detailed crystallizations conditions are given in **Supplementary Data** online. Data sets were integrated using MOSFLM and reduced using SCALA[38]. Molecular replacement and refinement were done using CNS version 1.1 (ref. 39) and figures were prepared using MolScript[40].

TmFtsZ T7 mutant structure. To disrupt the protofilament interaction in *T. maritima* FtsZ, several residues in the T7 loop were changed by ligating two PCR-amplified fragments. The product was cloned into vector pHis17, producing a C-terminally His_6-tagged protein with the T7 loop containing amino acids IRLTSRFARIE instead of INLDXXFADIE, starting at residue 217. The protein expressed well in C41 (ref. 41) cells after 4 h of 1 mM IPTG induction at 37 °C. Cells were opened by resuspending them in boiling water, followed by rapid addition of ice after 45 s. The protein was purified using Ni-NTA agarose and imidazole (300 mM at pH 6.0) and gel filtration (sephacryl S200, Amersham, in 20 mM Tris-HCl, 200 mM NaCl, 1 mM EDTA, 1 mM azide, pH 7.5). A total of 20 mg pure protein was obtained from 12 l of culture. Crystals were grown from 100 mM HEPES, pH 7.8, 24% (v/v) ethanol and 40 mM $MgCl_2$. A data set was collected on beamline 14.2 at the Synchrotron Radiation Source (SRS). The structure was solved by molecular replacement using the MjFtsZ structure (PDB entry 1FSZ).

Expression of TmFtsZ full length and N/C-terminal domains. Full length *T. maritima* FtsZ was cloned into vector pHis17 using genomic PCR, producing an untagged protein. The protein was purified by chromatography using Q-Sepharose (elution at ~350 mM NaCl, pH 7.5), hydroxyl apatite (Biorad, elution at ~200 mM phosphate, pH 7.5) and sephacryl S300 (Amersham) gel filtration in 20 mM Tris-HCl, 1 mM EDTA, 1 mM azide, pH 7.5. A total of 20 mg was obtained from 3 l of culture C41 cells.

Thermotoga maritima FtsZ N- and C-terminal domains (residues 22–190 and 188–336, respectively) were PCR-amplified from genomic DNA. Fragments were cloned into pHis17, adding eight additional residues at the C terminus: GSHHHHHH. Plasmids were transformed into C41 cells[41] and proteins from expression cultures (1 mM IPTG for 7 h at 25 °C) were purified with Ni-NTA and gel filtration as described for TmFtsZ T7 above. The N-terminal domain was eluted in 20 mM Tris-HCl, 200 mM NaCl, 1 mM EDTA and 1 mM azide, pH 7.5, and 15 mg was obtained from 12 l of culture. The C-terminal domain was eluted in 20 mM Tris-HCl, 1 mM EDTA and 1 mM azide, pH 7.5, and 20 mg was obtained from 12 l of culture. Electrospray mass spectrometry showed the proteins to be correct (N-terminal domain is 19,194 Da and should be 19,193 Da; C-terminal domain is 17,622 Da and should be 17,621 Da).

Table 1 Data collection and refinement statistics

	MjFtsZ, GMPCPP	MjFtsZ W319Y, GTP	TmFtsZ T7, GMPCPP	MjFtsZ refolded, empty	MjFtsZ refolded, GTP	MjFtsZ refolded, MgGTP
Data collection						
Space group	$I2_13$	$P1$	$P2_12_12$	$P2_1$	$P2_1$	$P2_1$
Cell dimensions						
a (Å)	161.1	114.0	61.0	70.1	70.3	70.4
b (Å)	161.1	114.3	66.8	53.9	55.2	55.2
c (Å)	161.1	115.1	181.5	89.2	88.1	88.1
α (°)		90.1				
β (°)		90.2		91.3	91.0	91.3
γ (°)		119.9				
Resolution (Å)	2.5	3.0	2.0	2.7	2.2	2.4
Completeness (%)[a]	98.9 (99.2)	94.7 (86.6)	99.5 (100.0)	99.9 (99.9)	98.2 (98.2)	95.9 (95.9)
R_{sym}[a]	0.063 (0.225)	0.084 (0.361)	0.065 (0.215)	0.079 (0.407)	0.071 (0.357)	0.070 (0.360)
Refinement						
R_{work}[a]	0.221 (0.346)	0.264 (0.492)	0.203 (0.234)	0.216 (0.286)	0.209 (0.237)	0.218 (0.282)
R_{free}[a,b]	0.253 (0.403)	0.298 (0.518)	0.234 (0.290)	0.296 (0.358)	0.259 (0.268)	0.264 (0.332)
No. atoms						
Protein	2,504	22,167	4,824	5,159	4,959	4,959
Water	95	676	367	122	247	247
Mg	1					
Ligand/ion	1	9	2	1	1	1
B-factors (Å^2)[c]						
Average	56.8	48.7	24.9	48.6	37.9	39.4
Bonded	1.86	4.67	3.00	3.22	4.6	3.36
R.m.s. deviations						
Bond lengths (Å)	0.012	0.011	0.005	0.007	0.006	0.007
Bond angles (°)	1.62	1.56	1.18	1.341	1.195	1.196

[a]Values in parentheses are for the highest-resolution shell. [b]For determination of R_{free}, 5% of reflections were randomly selected before refinement. [c]Temperature factors averaged for all atoms and r.m.s. deviation of temperature factors between bonded atoms.

TmFtsZ N- and C-terminal domains. CD spectra were recorded in a Jasco 720-715 spectropolarimeter using a 0.1-mm cell at 25 °C. Four scans for each sample or buffer were averaged. CD data (millidegrees) were reduced to mean residue ellipticity values (degrees cm^2 dmol^{-1}) with the manufacturer's Jasco J700 software.

GTPase assays were done as described[42]: 1 ml of 5.72% (w/v) ammonium molybdate in 6 N HCl, 1 ml 2.32% (w/v) polyvinyl alcohol, 2 ml 0.081% (w/v) malachite green and 2 ml of water were mixed and 200 µl was added to 50-µl reactions containing proteins or inorganic phosphate standards. Reactions contained 2 nmol of each protein and 1 mM GTP, pH 7, 2 mM magnesium, and were incubated for 20 min at 50 °C. Reactions were adjusted to 1 ml and read out at 630 nm.

For EM, reactions identical to the ones used in the GTPase assays were used with 2 nmol of protein. However, the incubation time at 50 °C was 5–10 min. Samples were transferred to glow-discharged copper EM grids and stained with uranyl acetate.

Refolded MjFtsZ without nucleotide. Large-scale refolding of *M. jannaschii* was carried out as follows: MjFtsZ was produced from the previously described expression plasmid[6] in 12 l of C41 cells[41]. Cells were resuspended in 300 ml of 50 mM Tris-HCl, 6 M urea, pH 7.0. After sonication and ultracentrifugation 135,000*g* the His_6-tagged FtsZ protein was purified using Ni-NTA agarose and imidazole under denaturing conditions (6 M urea). The purified, denatured protein was then diluted into 5 l of 50 mM Tris-HCl, 100 mM NaCl, pH 7.0, over several hours with rapid stirring. The refolded protein was then precipitated with 50% (saturated) ammonium sulfate and gel-filtrated using a sephacryl S300 column (Amersham) in 20 mM Tris-HCl, 1 mM EDTA, 1 mM azide, pH 7.5. To test for bound nucleotide, FtsZ was precipitated using 0.5 N cold $HClO_4$, and after centrifugation nucleotide absence in the supernatant was checked spectrophotometrically. A total of 16 mg refolded, nucleotide-free protein was obtained from 12 l.

MjFtsZ dimer structure and nucleotide soaks. Refolded, nucleotide-free MjFtsZ-GSHHHHHH was crystallized using 100 mM Tris-HCl, 200 mM Li_2SO_4, 40% (w/v) PEG400, pH 8.4. Data sets were collected on beamline ID29 at the European Synchrotron Radiation Facility (ESRF). For nucleotide soaks, crystals were incubated in mother liquor, supplemented with 3 mM GTP or 3 mM GTP with 6 mM magnesium chloride for 10 min. Structures were solved by molecular replacement using the MjFtsZ (PDB entry 1FSZ) structure.

MjFtsZ–MgGMPCPP structure. The original *M. jannaschii* FtsZ-GSHHHHHH crystals[6] were soaked with GMPCPP. Single crystals were transferred into 25% (w/v) PEG400, 0.07 M MES, pH 6.62, 4.5% (v/v) ethanol, 0.8 mM GMPCPP, 1.5 mM $MgCl_2$, and were incubated for 3–4 h. Crystals were then frozen using mother liquor plus 25% (w/v) PEG200 and a data set was collected on beamline 9.6 at the SRS.

MjFtsZ GTPase-deficient W319Y mutant. The untagged protein was expressed and purified as described with ~98% GTP bound[10]. Crystals were grown using 100 mM HEPES, pH 7.4, 1.3 M LiCl. A data set was collected on beamline BM14 at the ESRF. The structure was solved by molecular replacement using the MjFtsZ structure (PDB entry 1FSZ).

Coordinates. Structures and their corresponding structure factors have been deposited in the Protein Data Bank with the following accession codes: 1W58, MjFtsZ with GMPCPP soaked in; 1W5E, MjFtsZ W319Y mutant; 1W5F, TmFtsZ T7 mutant; 1W59, refolded MjFtsZ dimer, empty; 1W5B, refolded MjFtsZ dimer with GTP soaked in; 1W5A, refolded MjFtsZ dimer with MgGTP soaked in.

Note: Supplementary information is available on the Nature Structural & Molecular Biology website.

COMPETING INTERESTS STATEMENT
The authors declare that they have no competing financial interests.

ACKNOWLEDGMENTS
We thank the Ministerio de Ciencia y Tecnologia, Spain for financial support to M.A. We also thank J.M. Andreu (Madrid) for supplying us with the MjFtsZ-W319Y plasmid. Finally, we had great support on the following beamlines: Synchtrotron Radiation Source (14.2 and 9.6) and European Synchrotron Radiation Facility (ID29 and BM14).

Received 24 June; accepted 1 October 2004
Published online at http://www.nature.com/nsmb/

1. Errington, J., Daniel, R.A. & Scheffers, D.J. Cytokinesis in bacteria. *Microbiol. Mol. Biol. Rev.* **67**, 52–65 (2003).
2. Lutkenhaus, J. & Addinall, S.G. Bacterial cell division and the Z ring. *Annu. Rev. Biochem.* **66**, 93–116 (1997).
3. Rothfield, L., Justice, S. & Garcia-Lara, J. Bacterial cell division. *Annu. Rev. Genet.* **33**, 423–448 (1999).
4. Addinall, S.G. & Holland, B. The tubulin ancestor, FtsZ, draughtsman, designer and driving force for bacterial cytokinesis. *J. Mol. Biol.* **318**, 219–236 (2002).
5. Erickson, H.P. FtsZ, a prokaryotic homolog of tubulin? *Cell* **80**, 367–370 (1995).
6. Löwe, J. & Amos, L.A. Crystal structure of the bacterial cell-division protein FtsZ. *Nature* **391**, 203–206 (1998).
7. Nogales, E., Wolf, S.G. & Downing, K.H. Structure of the alpha beta tubulin dimer by electron crystallography. *Nature* **391**, 199–203 (1998).
8. Nogales, E., Downing, K.H., Amos, L.A. & Löwe, J. Tubulin and FtsZ form a distinct family of GTPases. *Nat. Struct. Biol.* **5**, 451–458 (1998).
9. Nogales, E., Whittaker, M., Milligan R.A. & Downing, K.H. High-resolution model of the microtubule. *Cell* **96**, 79–88 (1999).
10. Oliva, M.A. *et al.* Assembly of archaeal cell division protein FtsZ and a GTPase-inactive mutant into double-stranded filaments. *J. Biol. Chem.* **278**, 33562–33570 (2003).
11. Erickson, H.P., Taylor, D.W., Taylor, K.A. & Bramhill, D. Bacterial cell division protein FtsZ assembles into protofilament sheets and minirings, structural homologs of tubulin polymers. *Proc. Natl. Acad. Sci. USA* **93**, 519–523 (1996).
12. Löwe, J. & Amos, L.A. Tubulin-like protofilaments in Ca^{2+}-induced FtsZ sheets. *EMBO J.* **18**, 2364–2371 (1999).
13. Scheffers, D.J., de Wit, J.G., den Blaauwen, T. & Driessen, A.J. Substitution of a conserved aspartate allows cation-induced polymerization of FtsZ. *FEBS Lett.* **494**, 34–37 (2001).
14. Cordell, S.C., Robinson, E.J. & Löwe, J. Crystal structure of the SOS cell division inhibitor SulA and in complex with FtsZ. *Proc. Natl. Acad. Sci. USA* **100**, 7889–7894 (2003).
15. Romberg, L. & Mitchison, T.J. Rate-limiting guanosine 5′-triphosphate hydrolysis during nucleotide turnover by FtsZ, a prokaryotic tubulin homologue involved in bacterial cell division. *Biochemistry* **43**, 282–288 (2004).
16. Mitchison, T. & Kirschner, M. Dynamic instability of microtubule growth. *Nature* **312**, 237–242 (1984).
17. Mingorance, J., Rueda, S., Gomez-Puertas, P., Valencia, A. & Vicente, M. *Escherichia coli* FtsZ polymers contain mostly GTP and have a high nucleotide turnover. *Mol. Microbiol.* **41**, 83–91 (2001).
18. Huecas, S. & Andreu, J.M. Energetics of the cooperative assembly of cell division protein FtsZ and the nucleotide hydrolysis switch. *J. Biol. Chem.* **278**, 46146–46154 (2003).
19. Mukherjee, A. & Lutkenhaus, J. Guanine nucleotide-dependent assembly of FtsZ into filaments. *J. Bacteriol.* **176**, 2754–2758 (1994).
20. Bramhill, D. & Thompson, C.M. GTP-dependent polymerization of *Escherichia coli* FtsZ protein to form tubules. *Proc. Natl. Acad. Sci. USA* **91**, 5813–5817 (1994).
21. Ben-Yehuda, S. & Losick, R. Asymmetric cell division in *B. subtilis* involves a spiral-like intermediate of the cytokinetic protein FtsZ. *Cell* **109**, 257–266 (2002).
22. Lu, C., Reedy, M. & Erickson, H.P. Straight and curved conformations of FtsZ are regulated by GTP hydrolysis. *J. Bacteriol.* **182**, 164–170 (2000).
23. Diaz, J.F. *et al.* Activation of cell division protein FtsZ. Control of switch loop T3 conformation by the nucleotide γ-phosphate. *J. Biol. Chem.* **276**, 17307–17315 (2001).
24. Andreu, J.M., Oliva, M.A. & Monasterio, O. Reversible unfolding of FtsZ cell division proteins from archaea and bacteria. Comparison with eukaryotic tubulin folding and assembly. *J. Biol. Chem.* **277**, 43262–43270 (2002).
25. Löwe, J., Li, H., Downing, K.H. & Nogales, E. Refined structure of α β-tubulin at 3.5 Å resolution. *J. Mol. Biol.* **313**, 1045–1057 (2001).
26. Hyman, A.A., Chretien, D., Arnal, I. & Wade, R.H. Structural changes accompanying GTP hydrolysis in microtubules: information from a slowly hydrolyzable analogue guanylyl-(α,β)-methylene-diphosphonate. *J. Cell Biol.* **128**, 117–125 (1995).
27. Nogales, E., Whittaker, M., Milligan, R.A. & Downing, K.H. High-resolution model of the microtubule. *Cell* **96**, 79–88 (1999).
28. Huecas, S. & Andreu, J.M. Polymerization of nucleotide-free, GDP- and GTP-bound cell division protein FtsZ: GDP makes the difference. *FEBS Lett.* **569**, 43–48 (2004).
29. Ravelli, R.B. *et al.* Insight into tubulin regulation from a complex with colchicine and a stathmin-like domain. *Nature* **428**, 198–202 (2004).
30. Nogales, E., Wang, H.W. & Niederstrasser, H. Tubulin rings: which way do they curve? *Curr. Opin. Struct. Biol.* **13**, 256–261 (2003).
31. Scheffzek, K. *et al.* The Ras–RasGAP complex: structural basis for GTPase activation and its loss in oncogenic Ras mutants. *Science* **277**, 333–338 (1997).
32. Daumke, O., Weyand, M., Chakrabarti, P.P., Vetter, I.R. & Wittinghofer, A. The GTPase-activating protein Rap1GAP uses a catalytic asparagine. *Nature* **429**, 197–201 (2004).
33. Schindelin, H., Kisker, C., Schlessman, J.L., Howard, J.B. & Rees, D.C. Structure of ADP x AlF_4(–)-stabilized nitrogenase complex and its implications for signal transduction. *Nature* **387**, 370–376 (1997).
34. Egea, P.F. *et al.* Substrate twinning activates the signal recognition particle and its receptor. *Nature* **427**, 215–221 (2004).
35. Focia, P.J., Shepotinovskaya, I.V., Seidler, J.A. & Freymann, D.M. Heterodimeric GTPase core of the SRP targeting complex. *Science* **303**, 373–377 (2004).
36. Tesmer, J.J., Berman, D.M., Gilman, A.G. & Sprang, S.R. Structure of RGS4 bound to AlF_4-activated $G_{i\alpha1}$: stabilization of the transition state for GTP hydrolysis. *Cell* **89**, 251–261 (1997).
37. Stock, D., Perisic, O. & Löwe, J. Nanolitre crystallisation at the MRC Laboratory of Molecular Biology. *Prog. Biophys. Mol. Biol.* (in the press).
38. Collaborative Computational Project, Number 4. The CCP4 suite: programs for protein crystallography. *Acta Crystallogr. D* **50**, 760–763 (1994).
39. Brunger, A.T. *et al.* Crystallography & NMR system: a new software suite for macromolecular structure determination. *Acta Crystallogr. D* **54**, 905–921 (1998).
40. Kraulis, P.J. MOLSCRIPT: a program to produce both detailed and schematic plots of protein structures. *J. Appl. Crystallogr.* **24**, 946–950 (1991).
41. Miroux, B. & Walker, J.E. Over-production of proteins in *Escherichia coli*: Mutant hosts that allow synthesis of some membrane proteins and globular proteins at high levels. *J. Mol. Biol.* **260**, 289–298 (1996).
42. Henkel, R.D., van de Berg, J.L. & Walsh, R.A. A microassay for ATPase. *Anal. Biochem.* **169**, 312–318 (1987).